Kinetics of Liquid-Phase Condensation of Propylene with Formaldehyde over H–MFI and H–BEA Zeolites

S. P. Bedenko[a],*, K. I. Dement'ev[a], and V. F. Tret'yakov[a],†

[a] *Topchiev Institute of Petrochemical Synthesis, Russian Academy of Sciences, Moscow, 119991 Russia*
*e-mail: bedenko@ips.ac.ru

Abstract—This study investigated the kinetic patterns of the liquid-phase Prins condensation of propylene with formaldehyde in the range of 120–180°C over H–MFI and H–BEA zeolites. The apparent reaction order with respect to formaldehyde was found to vary between 0.1 and 0.2 for H–BEA and to be close to zero for H–MFI. The apparent activation energy for H–MFI and H–BEA was 26.1±0.6 kJ/mol and 20.0±4.0 kJ/mol, respectively. Based on these results, the reaction was demonstrated to occur in the intradiffusion or transition region; the calculated Thiele modulus and effectiveness factor further confirmed this fact. The diffusion limitations were partially removed by raising the initial formaldehyde concentration, as indicated by an increase in the apparent order of formaldehyde conversion to 1.0 for H–BEA and to 0.4 in the H–MFI case. To describe the substrate transformations observed, a modernized reaction mechanism was proposed.

Keywords: Prins reaction, kinetics, propylene, formaldehyde, MFI, BEA

The Prins reaction provides an alternative approach for the production of valuable petrochemicals such as dienes. The steadily growing interest in this reaction in recent years can be explained by its easy integration into the chemical bonding process of carbon dioxide [1]: methanol generated as a primary product of CO_2 conversion then transforms into olefins and formaldehyde, which are precursors for the Prins reaction [2–5]. This reaction is traditionally catalyzed by various homogeneous acid catalysts (e.g., sulfuric acid, orthophosphoric acid, $ZnCl_2$, or $SnCl_4$), which lead to major process challenges and have a relatively high environmental impact. The environmental impact is caused by significant amounts of wastewater, equipment corrosion, and complicated control over process selectivity, all being notoriously associated with the use of traditional homogeneous acid catalysts [6]. To overcome these issues, a significant number of recent studies have investigated various solid acids [7–11], in particular zeolites [12–21], as catalysts for the Prins reaction.

A major challenge for the liquid-phase Prins reaction is its selectivity control: depending on specific reaction conditions and solvents, the reaction produces 4-substituted-1,3-dioxanes, γ-unsaturated alcohols, or 3-substituted-1,3-diols [22, 23]. The condensation products of lower olefins with formaldehyde in non-aqueous solvents consist of γ-unsaturated alcohols, their downstream conversion products (e.g., dienes and derivatives of dihydro-2*H*-pyran and tetrahydro-2*H*-pyran), and 4-substituted-1,3-dioxanes, whereas almost no 3-substituted-1,3-diols are formed [16, 17, 19, 21]. In the Prins reaction, the selectivity of zeolite catalysts is primarily affected by their physicochemical (particularly acidic and textural) properties and the residence time of the reactants. While the effects of the physicochemical properties of a number of zeolites have been studied to some extent in the above references, the Prins reaction kinetics in the presence of heterogeneous catalysts remains essentially unexplored. The several scattered publications on this subject are limited to DFT simulations of formaldehyde–propylene interactions in the presence of various heterogeneous catalysts [24–27] and a study

---

† Deceased.

into the kinetics of the gas-phase Prins reaction in the presence of heteropolyacids [28].

The purpose of the present study was to investigate the kinetic patterns of the liquid-phase Prins condensation of propylene with formaldehyde in a 1,4-dioxane medium over H–MFI and H–BEA zeolites to assess the feasibility of kinetic control in the range of 120–180°C.

EXPERIMENTAL

MFI and BEA zeolites manufactured by Zeolyst International, specifically CBV 3024E (Si/Al = 15) and CP814E* (Si/Al = 12.5), respectively, were used as catalysts. Prior to testing, a protonic form of the samples was prepared by air calcination at 500°C for 12 h. The physicochemical properties of these catalysts are detailed in [21]. The particle size of zeolite powders was evaluated by dynamic light scattering (DLS) [29]. Both samples were found to have a unimodal particle size distribution with a maximum of 0.8 μm for H–MFI and 1.9 μm for H–BEA.

Kinetic tests were carried out in a 50 mL stainless steel autoclave reactor under stirring (600 rpm) in 1,4-dioxane, a traditional solvent for this reaction [16, 17, 19, 21, 30]. For this stirring speed, we had experimentally confirmed (in advance) that the reactant diffusion in the solvent bulk affected neither the formaldehyde conversion nor the product selectivity. The stirring speed was shown to have no effect on the rate of substrate conversion (Fig. 1). Before the test, 0.25 g of the catalyst sample, 0.5–2.0 g of paraformaldehyde, and the 1,4-dioxane solvent were placed in an autoclave. The autoclave was then closed, purged with an inert gas to remove air, and filled with propylene, the amount of which being constantly maintained at 6.5 g. The reaction time was varied between 0.25 and 2.0 h to reduce the effect of catalyst deactivation on the test results. The reaction was carried out at autogenous pressure. During the reaction, samples were taken every 0.25 h (15 minutes) and analyzed using a Chromatec Crystal 2000M gas chromatograph equipped with a 50 m × 0.32 mm SE-54 column and a flame ionization detector.

The test data were processed using Statistica 12 and Microsoft Excel software.

RESULTS AND DISUSSION

For Prins condensation of propylene with formaldehyde in the presence of heterogeneous catalysts, researchers
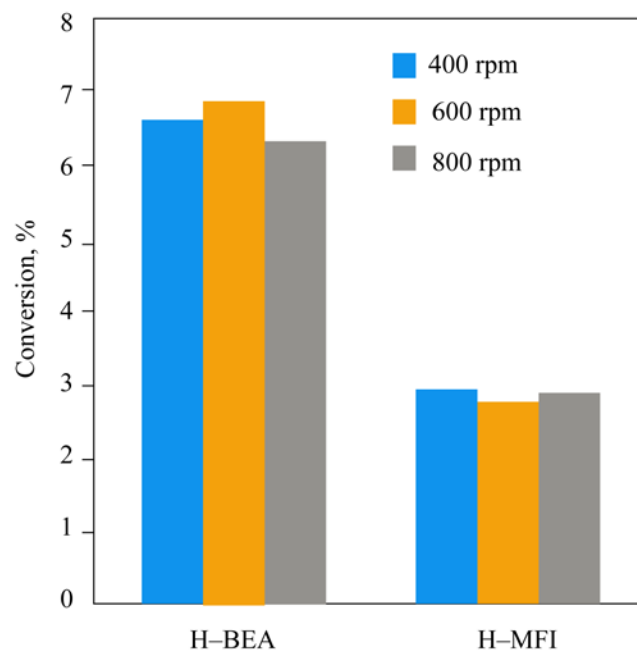
Fig. 1. Formaldehyde conversion over H–BEA and H–MFI as a function of stirring speed. Reaction conditions: CH_2O concentration 1.587 mol/L; 150°C; reaction time 0.25 h.

have proposed a number of conversion routes differing in the combinations of products and chemical reactions [16, 21, 28]. Nonetheless, all routes that involve reactions occurring in gas phases or non-aqueous solvents are commonly considered to generate γ-unsaturated alcohol as a primary product to be dehydrated into target diene. Moreover, diene is also an intermediate capable of entering into condensation reactions with formaldehyde to generate cyclic oxygen-containing products.

In all our experiments, the propylene conversion did not exceed 10%. This suggests a large excess of propylene remaining in all experimental points. A decline in the olefin to formaldehyde ratio is known to increase the 4-substituted-1,3-dioxane selectivity, thus compromising the potential production of buta-1,3-diene or its desired precursor (but-3-en-1-ol) [16]. Therefore, it is inexpedient to decrease the propylene partial pressure in this process. Logically enough, we described the relevant reactions by equations that disregarded variations in the propylene concentration.

Kinetic patterns in the presence of H–BEA. While BEA-type zeolites have proven to be the most selective to dienes in liquid-phase reactions, they promote significant generation of undesirable by-products such as

Table 1. Initial rates of formaldehyde consumption and product formation over H-BEA

C_f^0	T, C	Initial concentration change rate $\times 10^2$, mol L^{-1} h^{-1}							
		CH$_2$O	(but-3-en-1-ol) OH	(aldehyde) O	(cis-enol) OH	(3,6-dihydro-2H-pyran) O	(4-methyl-1,3-dioxane) O,O	(4-hydroxytetrahydro-2H-pyran) OH,O	(butadiene)
1.587	150	−42.63	1.84	1.20	0.19	13.26	3.89	1.41	2.28
1.587	150	−44.62	2.00	1.16	0.20	13.96	3.86	1.50	2.62
1.587	150	−40.56	1.89	1.10	0.17	13.44	3.72	1.36	2.40
0.794	150	−31.93	0.95	0.57	0.09	6.55	2.38	3.04	6.28
3.174	150	−81.89	3.75	2.26	0.36	26.42	9.86	0.83	1.32
1.587	120	−25.78	0.80	0.80	0.06	7.07	2.79	0.94	2.48
1.587	135	−31.95	1.25	0.92	0.10	8.69	3.53	1.19	2.97
1.587	165	−49.23	2.08	1.20	0.23	14.15	4.55	2.11	4.24
1.587	180	-55.47	2.60	1.34	0.27	15.98	4.84	2.61	4.47

3,6-dihydro-2H-pyran, 4-hydroxytetrahydro-2H-pyran, and 4-methyl-1,3-dioxane, along with a target reaction product [16, 21]. Table 1 presents the initial change rates of the feedstock and product concentrations evaluated by extrapolation. The highest formation rate was observed for 3,6-dihydro-2H-pyran and 4-methyl-1,3-dioxane, which may indicate that these compounds were not converted under the reaction conditions.

On the other hand, under the same conditions the formaldehyde concentration declined almost linearly over time (Fig. 2a), whereas the kinetic curves for $\ln(C/C_0)$–t were found to be highly nonlinear (Fig. 2b). It would be fair to assume a zero or near-zero order of the condensation reaction with respect to formaldehyde. To test this hypothesis, the data were approximated by the equation:

$$\frac{dC_f}{dt} = -kC_f^n,$$

where n is the reaction order; k is the reaction rate constant; and C_f is the formaldehyde concentration.

In an integral form, this equation appears as follows:

$$C_f^{1-n} = C_{f0}^{1-n} - (1-n)kt.$$

The reaction order and rate constant were derived from the integral equation using the Levenberg–Marquardt least squares algorithm. In the absence of the disregarded factors, the adequacy of the model description was double-controlled by an analysis of regression residuals, with homoscedasticity requirement to be satisfied.

In all the cases, the reaction order was fractional, between 0.1 and 0.2 (Table 2). The activation energy amounted to about 20.0±4.0 kJ/mol. The patterns observed indicate major diffusion limitations in the system, with the reaction likely occurring in the intradiffusion region. In all probability, this occurrence, typical of zeolite catalysts, is associated with their porous structure [31, 32]. The kinetic curves of product formation showed that the change rate of the product concentration is also essentially time-independent, thus confirming the assumption of inhibited diffusion.

The contribution of diffusion limitations to the condensation process was evaluated in a series of experiments at different initial formaldehyde concentrations under equal conditions. The kinetic curves (Fig. 3) indicate that an increase in the initial concentration (with other conditions being equal) affects the reaction order. Moreover, at an initial concentration of 3.174 mol/L the order equals 1.0, which meets the expected value (Table 3) and agrees with the available
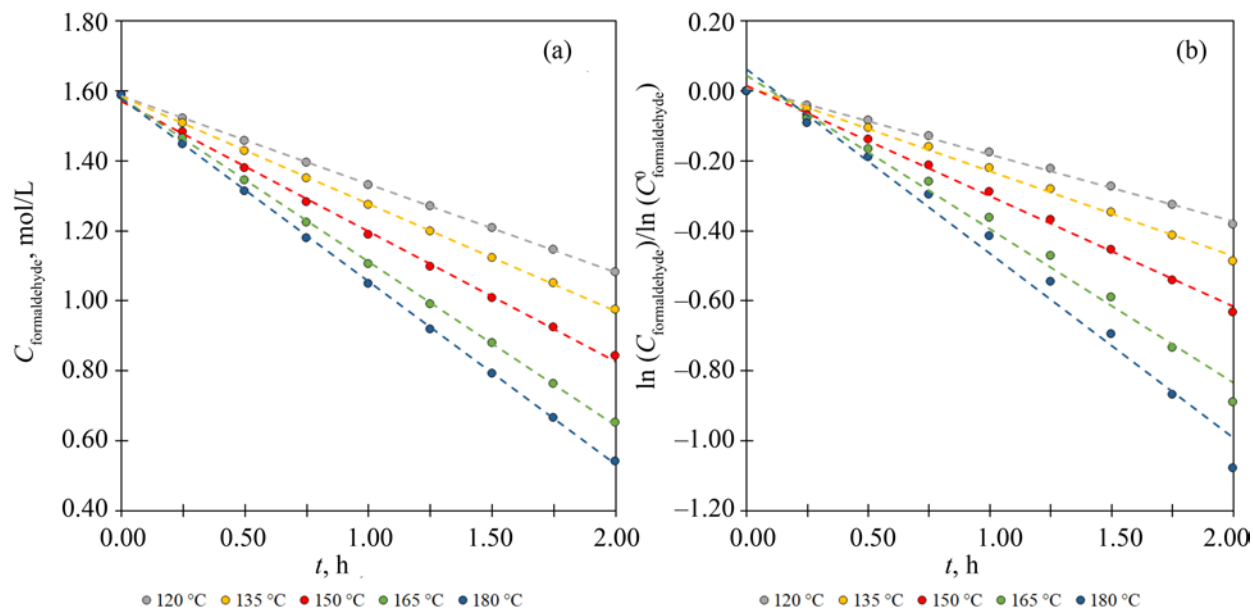
Fig. 2. Formaldehyde concentration curves for H–BEA at different temperatures. Coordinate systems: (a) C_f–t and (b) $\ln(C/C_0)$–t.

data on the kinetics of nopol synthesis by the Prins reaction over a heterogeneous catalyst [33]. In all likelihood, a growth in the initial concentration increases the reactant diffusion flux and partially removes the diffusion limitations, which may serve as evidence of external diffusion limitations. However, the independence of the degree of conversion from the stirring speed, as demonstrated by our preliminary test, indicates that no such limitations exist. Although this contradiction may be indicative of the reaction occurrence in the transition region, it is difficult to identify the exact region of reaction occurrence under the given conditions.

Table 2. Kinetic constants of propylene–formaldehyde condensation over H–BEA at different temperatures (C_f^0 = 1.587 mol/L)

T, °C	Rate constant	Reaction order	Apparent activation energy, kJ/mol	Pre-exponental factor
120	0.240 ± 0.050 mol$^{0.9}$ h^{-1} L$^{-0.9}$	0.12 ± 0.07		
135	0.292 ± 0.002 mol$^{0.8}$ h^{-1} L$^{-0.8}$	0.19 ± 0.03		
150	0.334 ± 0.004 mol$^{0.6}$ h^{-1} L$^{-0.6}$	0.42 ± 0.04	20.0 ± 4.0	102 ± 3
165	0.463 ± 0.002 mol$^{0.9}$ h^{-1} L$^{-0.9}$	0.12 ± 0.02		
180	0.522 ± 0.001 mol$^{0.9}$ h^{-1} L$^{-0.9}$	0.12 ± 0.02		

Table 3. Kinetic constants of propylene–formaldehyde condensation over H–BEA at 150°C

Initial formaldehyde concentration, mol/L	Rate constant	Reaction order
0.794	0.333 ± 0.003 mol$^{0.8}$ h^{-1} L$^{-0.2}$	0.23 ± 0.02
1.587	0.334 ± 0.004 mol$^{0.6}$ h^{-1} L$^{-0.6}$	0.42 ± 0.04
3.174	0.256 ± 0.002 h^{-1}	1.0^a

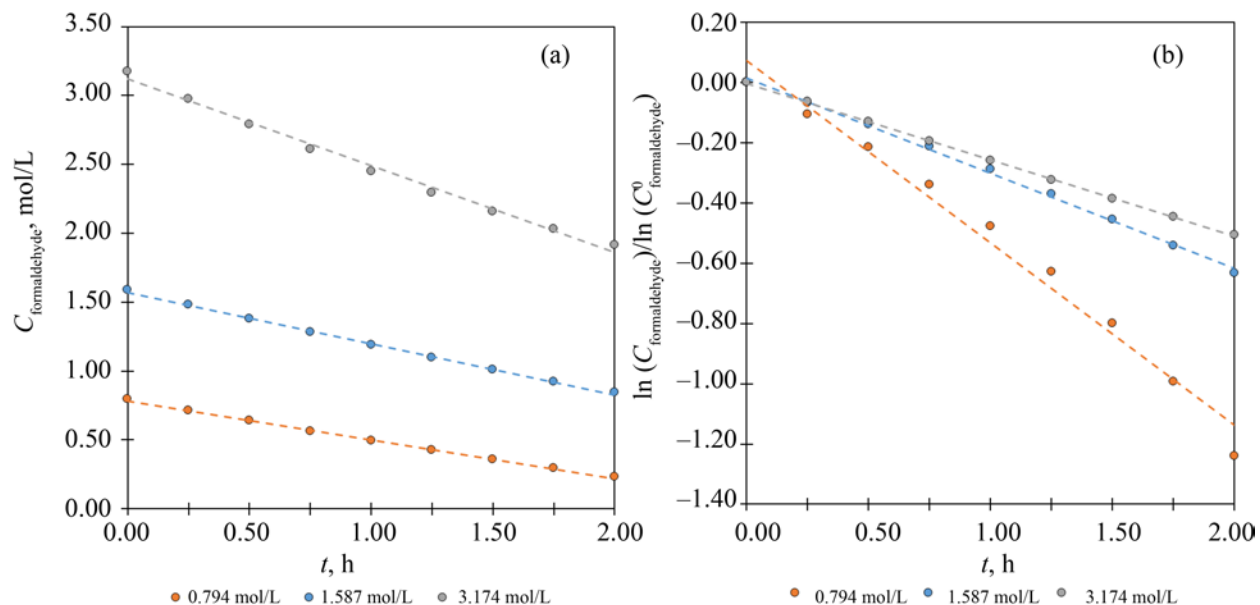^{a} At $n = 1$, the following equation was used $C_f = C_f^0 e^{-kt}$.

Fig. 3. Formaldehyde concentration curves for different initial concentrations in presence of H–BEA (at 150°C). Coordinate systems: (a) C_f–t and (b) $\ln(C/C_0)$–t.

The kinetic data for the reaction products enabled us to determine that, at an initial formaldehyde concentration of 3.174 mol/L, the reaction order of but-3-en-1-ol, *n*-butanal, and but-2-en-1-ol formation also equals 1.0 and adheres to the following equation (see also Fig. 4):

$$C_i = \frac{k_i}{k_f}\left(C_{f0} - C_f\right).$$

The calculated rate constants of the formation of primary reaction products and their ratio to the rate constant of formaldehyde consumption are presented in Table 4. The small rate constants of product formation with respect to those of formaldehyde consumption are probably due to the vigorous consumption of primary products during subsequent reactions to produce buta-1,3-diene and 4-hydroxytetrahydro-2*H*-pyran. The formation of 4-methyl-1,3-dioxane is described with good accuracy when the apparent reaction order of 1.3 with respect to formaldehyde is assumed in the equation instead of the expected second order. Under the experimental conditions, some diffusion limitations likely continued for the diffusion of reaction products. For the same reason, we were unable to propose an adequate calculation model for the rate constants of secondary reaction products, namely buta-1,3-diene, 4-hydroxytetrahydro-2*H*-pyran, and 3,6-dihydro-2*H*-pyran.

The test data show that the highest formation rates of buta-1,3-diene and 4-hydroxytetrahydro-2*H*-pyran in the series with the most stringent diffusion limitations were achieved at an initial formaldehyde concentration of 0.794 mol/L. On the other hand, raising the initial

Table 4. Formation rate constants of primary products over H–BEA at 150°C and initial formaldehyde concentration of 3.174 mol/L

Reaction product	Reaction rate constant, $\times 10^2$ h^{-1}	k_i/k_f
But-3-en-1-ol	1.26±0.02	0.050
But-2-en-1-ol	0.121±0.002	0.005
n-Butanal	0.731±0.002	0.029
4-Methyl-1,3-dioxane	2.2±0.2[a]	0.085

[a] For 4-methyl-1,3-dioxane, the rate constant was measured in L$^{1.3}$ h^{-1} mol$^{-1.3}$.

concentration to 3.174 mol/L speeded up the formation of the final stable reaction products (i.e., *n*-butanal, 4-methyl-1.3-dioxane, and 3,6-dihydro-2*H*-pyran). This pattern opens a new approach for control over reaction selectivity, particularly for enhancing the yield of the target intermediates.

To assess the effect of diffusion limitations on H–BEA catalytic activity, the Thiele modulus and effectiveness factor were evaluated at various reaction temperatures. When calculating the diffusion coefficient, we assumed Knudsen diffusion in zeolite pores as the limiting stage of the entire process. The Thiele modulus was derived from transcendental equation (1), with a positive solution being taken as the parameter value. The effectiveness factor was evaluated by transcendental equation (2):

$$\frac{k_{f,t}}{V_{pore}} = \frac{D_{ef}}{L} M \frac{\exp^M - \exp^{-M}}{\exp^M + \exp^{-M}}, \qquad (1)$$

$$E = \frac{1}{M} \frac{\exp^M - \exp^{-M}}{\exp^M + \exp^{-M}}, \qquad (2)$$

where M is the Thiele modulus; E is the effectiveness factor factor; D_{ef} is the Knudsen diffusion coefficient (cm^2/s); $k_{f,t}$ is the apparent reaction rate (cm^2 g^{-1} s^{-1}); V_{pore} is the volume of catalyst pores (cm^3/g); and L is the effective pore depth (cm).

The evaluation results are presented in Table 5. Within the entire temperature range, the effectiveness factor is close to 1, which is indicative of a high degree of reaction inhibition as a result of formaldehyde diffusion to the active site.

These data show that but-3-en-1-ol, but-2-en-1-ol, *n*-butanal, and 4-methyl-1,3-dioxane are competing reaction products derived from a common intermediate; this intermediate is produced by addition of protonated formaldehyde to a propylene molecule. The ratio between the product formation rate constants reflects the preference of the intermediate's stabilization pathways. It is also reasonable to assume that buta-1,3-diene and 4-hydroxytetrahydro-2*H*-pyran are competing products derived from a common intermediate denoted as [ZX$_2$]$^+$. These intermediates can probably be formed both from but-3-en-1-ol and from but-2-en-1-ol. The reaction mechanism based on the kinetic curves is depicted in Fig. 5. The experimental data clearly show that, in
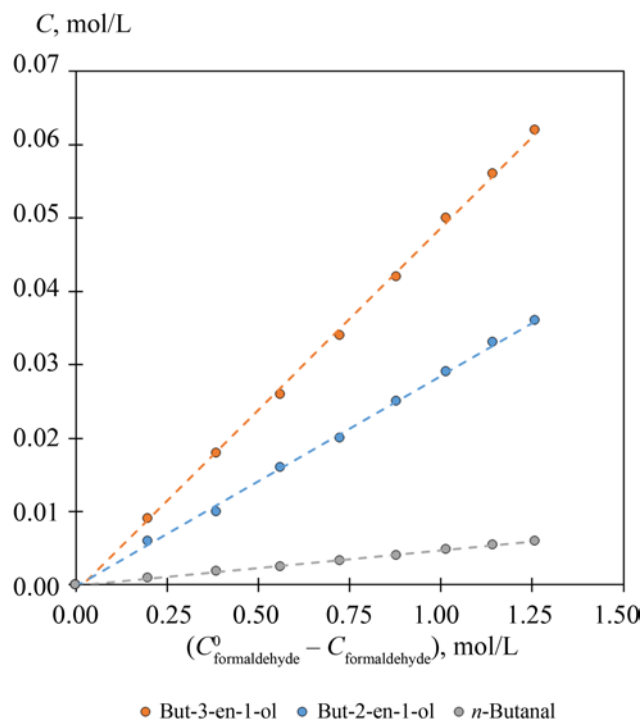
Fig. 4. Product concentrations as functions of formaldehyde consumption ($C_f^0 - C_f$) for H–BEA (at initial concentration of 3.174 mol/L).

this reaction system, *n*-butanal, 4-methyl-1,3-dioxane, and 3,6-dihydro-2*H*-pyran are final reaction products, while but-3-en-1-ol, but-2-en-1-ol, buta-1,3-diene, and 4-hydroxytetrahydro-2*H*-pyran are intermediates.

The reaction orders and reaction mechanism originated from our experiment and assessment were compared with the data reported in a study by Kots et al. [28], who investigated the patterns of gas-phase propylene–formaldehyde condensation in the presence of silica-supported heteropolyacid (HPA), specifically 24SiW.

Table 5. Thiele modulus and effectiveness factor at various temperatures with initial formaldehyde concentration of 1.587 mol/L

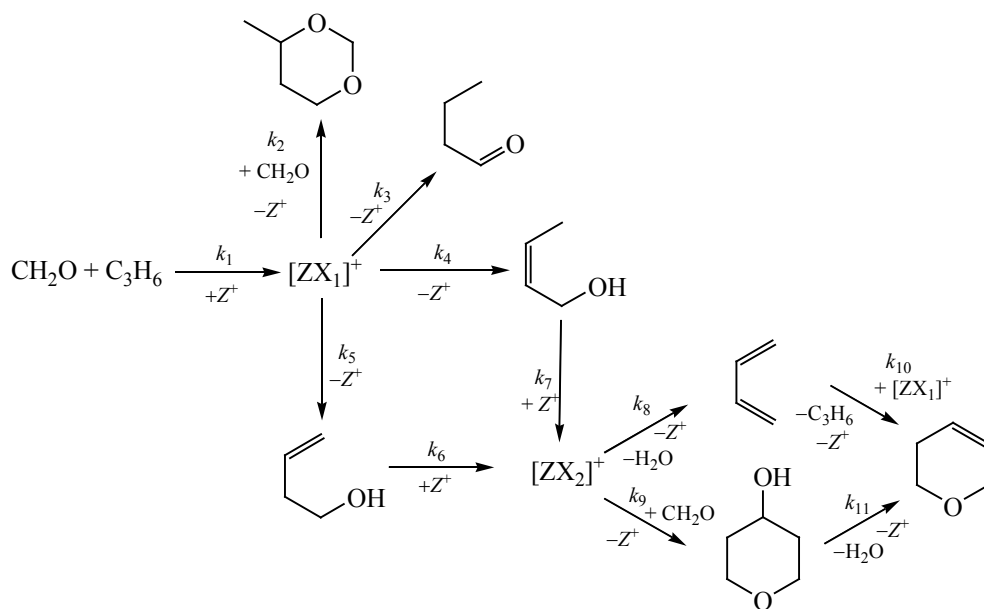| T, °C	M	E
120	0.155	0.992
135	0.172	0.990
150	0.186	0.987
165	0.221	0.984
180	0.238	0.982

Fig. 5. Suggested Prins condensation mechanism in non-aqueous solvent.

Their study proposes a number of models for the formation of two primary reaction products (*n*-butanal and buta-1,3-diene) and 2-methylene-butanal, a compound formed from the condensation of formaldehyde and *n*-butanal. The initial formaldehyde concentration was found to have almost no effect on the formation rate of the primary products, with close to pseudo-zero order of the reaction. However, the product formation rate has the first order with respect to propylene. The authors attributed this fact to formaldehyde's ability to oversaturate the active sites in HPAs, thus building a large excess of formaldehyde on the catalyst's active site. This phenomenon was also noted in a study by Schnee and Gaigneaux [34] focused on methanol dehydration to dimethyl ether. These researchers also detected neither but-1,3-diene precursors such as but-3-en-1-ol or but-2-en-1-ol, nor large molecules (e.g., 3,6-dihydro-2*H*-pyran or 4-hydroxytetrahydro-2*H*-pyran) in the reaction products. In a high-temperature gas-phase process, these products are likely subject to rapid transformations: but-3-en-1-ol or but-2-en-1-ol are Bodenstein intermediates during the formation of buta-1,3-diene, while 3,6-dihydro-2*H*-pyran and 4-hydroxytetrahydro-2*H*-pyran act as coke precursors, which is consistent with the data reported in [35].

Reaction kinetics in the presence of H–MFI. The MFI structural type is highly selective to γ-unsaturated alcohols, which are considered preferable precursors for dienes [16, 21]. Table 6 presents the initial rates of formaldehyde consumption and product formation derived from the product concentration curves. H–MFI slows down (compared to H–BEA) formaldehyde consumption and the formation of products with relatively large molecules (e.g., 3,6-dihydro-2*H*-pyran, 4-methyl-1,3-dioxane, and 4-hydroxytetrahydro-2*H*-pyran). Unlike H–BEA, with its markedly higher formation rate of large molecules, H–MFI promotes the formation of but-3-en-1-ol as the main product. These differences in the formaldehyde conversion and product formation rates are likely associated with the textural properties of the samples.

As in the H–BEA case, the formaldehyde concentration was found to be a linear function of reaction time in the C_f–t coordinates (Fig. 6a) and nonlinear in $\ln(C_f/C_f^0)$–t (Fig. 6b). On the other hand, a regression analysis of the experimental data showed the best results when the apparent reaction order was assumed to be zero. Table 7 presents the calculated rate constants at various temperatures. These rate constants for H–MFI proved to be almost half the values obtained for H–BEA. With both zeolites, the reaction rate is likely limited by internal

Table 6. Initial rates of formaldehyde consumption and product formation over H–MFI
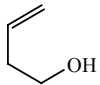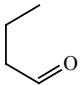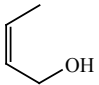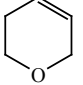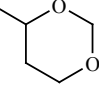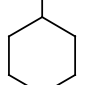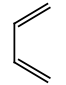
C_f^0	T, C	Initial concentration change rate $\times 10^2$, mol L^{-1} h^{-1}							
		CH$_2$O	(but-3-en-1-ol)	(n-butanal)	(but-2-en-1-ol)	(dihydropyran)	(4-methyl-dioxane)	(hydroxy-tetrahydropyran)	(butadiene)
1.587	150	−17.27	8.08	2.72	0.49	1.66	0.45	0.55	0.46
1.587	150	−17.67	8.47	2.93	0.54	1.65	0.46	0.51	0.44
1.587	150	−17.67	8.47	2.75	0.65	1.65	0.44	0.55	0.47
0.794	150	−10.80	3.19	1.21	0.25	0.98	0.27	1.24	1.10
3.174	150	−31.00	13.62	5.30	1.05	3.95	1.07	0.31	0.28
1.587	120	−9.39	3.25	1.34	0.34	1.28	0.27	0.27	0.33
1.587	135	−11.81	4.34	1.83	0.42	1.45	0.38	0.42	0.36
1.587	165	−22.52	9.30	3.06	0.59	2.62	0.83	0.85	0.79
1.587	180	−27.59	10.48	3.99	0.66	3.14	1.11	1.24	1.01

Table 7. Kinetic constants of propylene–formaldehyde condensation over H–MFI at different temperatures (C_f^0 = 1.587 mol/L)

T, °C	Rate constant, mol h^{-1} L^{-1}	Apparent activation energy, kJ/mol	Preexponential factor
120	0.0923±0.0003		
135	0.121±0.001		
150	0.156±0.005	26.1±0.6	268±1
165	0.206±0.004		
180	0.266±0.002		

diffusion in the catalyst pores. However, the pseudo-zero apparent reaction order in the H–MFI case obviously indicates stringent diffusion limitations in the system. The apparent activation energy for H–MFI was 26.1±0.6 kJ/mol versus 20±4 kJ/mol for H–BEA. In all probability, the different pore geometry hindered the reaction process and caused additional diffusion limitations for the substrate. At the same time, this low activation energy is typical of reactions in the diffusion region.

Figure 7 provides the kinetic curves for different initial concentrations of formaldehyde. In contrast to the H–BEA case, varying the initial concentration had no noticeable effect on the formaldehyde concentration curve. A regression analysis showed that the apparent reaction order was zero for initial concentrations of 0.794 and 1.587 mol/L, and 0.4 for 3.174 mol/L (Table 8). However, the low conversion caused by the lower catalytic activity of H–MFI added uncertainty when evaluating the reaction order.

In the presence of H–MFI, the formation rate constants of but-3-en-1-ol, *n*-butanal, and but-2-en-1-ol proved to be markedly higher than those with H–BEA (Table 9).

Attention should further be paid to the significant decrease in the formation rate constant of 4-methyl-

Table 8. Kinetic constants of propylene–formaldehyde condensation over H–MFI at 150°C

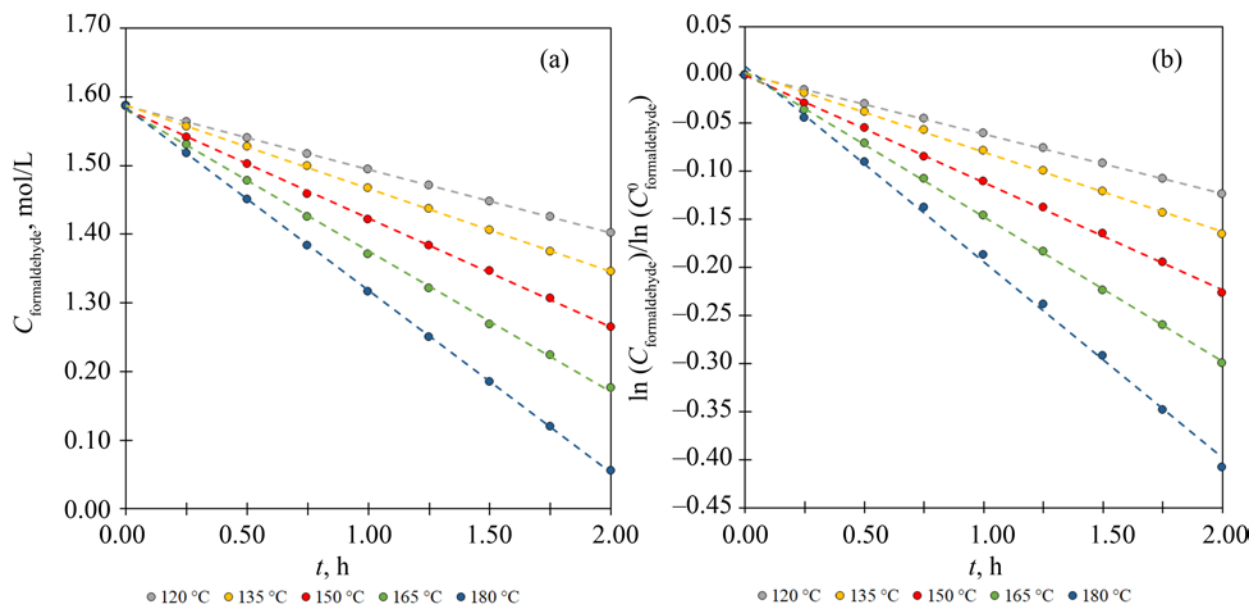| Initial formaldehyde concentration, mol/L	Rate constant	Reaction order
0.794	0.111±0.001 mol h^{-1} L^{-1}	0
1.587	0.156±0.005 mol h^{-1} L^{-1}	0
3.174	0.200±0.070 mol$^{0.6}$ h^{-1} L$^{-0.6}$	0.4±0.3

Fig. 6. Formaldehyde concentration curves for H–MFI at different temperatures. Coordinate systems: (a) C_f–t and (b) $\ln(C/C_0)$–t.
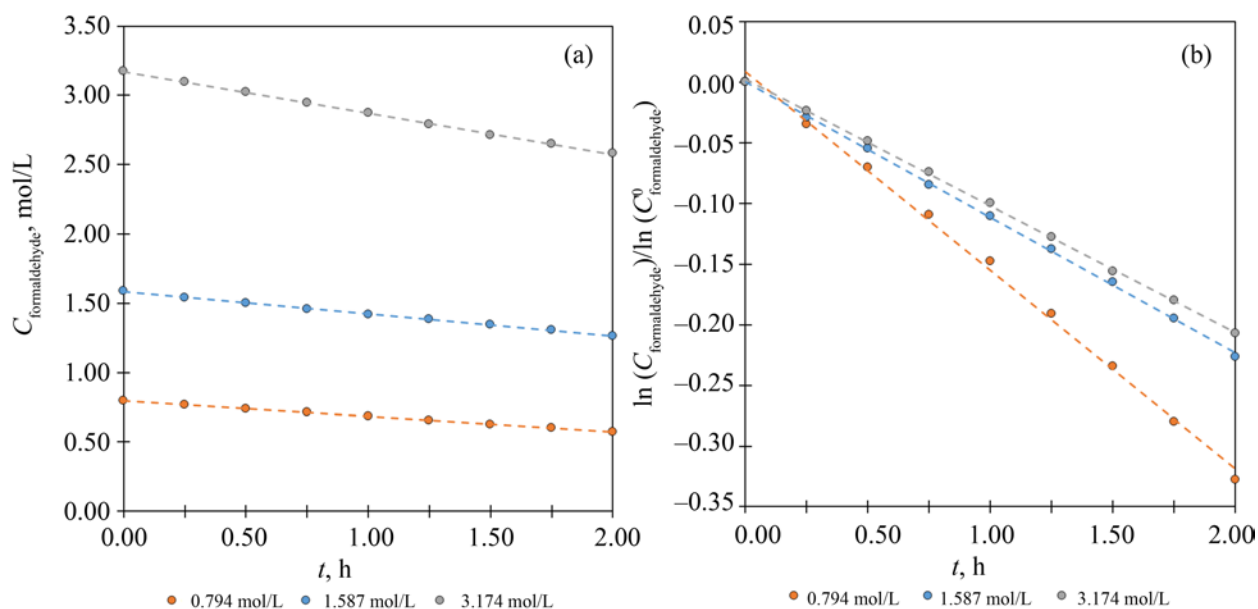

Fig. 7. Formaldehyde concentration curves for H–MFI for different initial concentrations (at 150°C). Coordinate systems: (a) C_f–t and (b) $\ln(C/C_0)$–t.

1.3-dioxane. A comparison of formation rate constants of primary products for the two zeolites suggests major suppression of secondary reactions over H–MFI. Therefore, changing the zeolite type is probably the most practicable method for controlling the Prins reaction selectivity because H–MFI has markedly higher selectivity to buta-1,3-diene precursors, whereas the formation of reaction products such as 4-methyl-1,3-dioxane is strongly limited by the H–MFI pore structure. The apparent reaction order for 4-methyl-1,3-dioxane over H–MFI is 0.6; this is still far from the theoretical

Table 9. Formation rate constants of primary products over H–MFI at 150°C and initial formaldehyde concentration of 3.174 mol/L

Reaction product	Reaction rate constant, 10^2 mol h^{-1} L^{-1}	k_i/k_f
But-3-en-1-ol	8.78±0.03	0.44
But-2-en-1-ol	0.670±0.005	0.03
n-Butanal	3.21±0.05	0.16
4-Methyl-1,3-dioxane	1.0±0.3^a	0.05

^{a} For 4-methyl-1,3-dioxane, the rate constant was measured in mol$^{0.4}$ h^{-1} L$^{0.4}$.

Table 10. Thiele modulus and effectiveness factor at various temperatures with initial formaldehyde concentration of 1.587 mol/L

T, °C	M	E
120	0.127	0.995
135	0.148	0.993
150	0.173	0.990
165	0.199	0.987
180	0.229	0.983

second order and indicates stringent diffusion limitations in its formation.

Table 10 provides the Thiele modulus and effectiveness factors calculated at different temperatures in a manner similar to that described above. As in the H–BEA case, the effectiveness factor of nearly 1.0 directly indicates strong reaction inhibition resulting from internal diffusion. Apparently, further studies into the effects of catalyst particle size and post-synthetic modifications (i.e., desilylation or recrystallization) on the activity of the sample are needed to effectively remove the diffusion limitations.

CONCLUSIONS

The kinetic patterns of propylene–formaldehyde condensation were investigated under typical Prins reaction conditions (including a 1.4-dioxane medium and the range of 120–180°C) in the presence of H–BEA and H–MFI. The first-order kinetic model was found to inadequately describe formaldehyde conversion because of diffusion limitations. Under these conditions, the apparent order of formaldehyde conversion was either close to pseudo-zero (0.1–0.2 for H–BEA) or equal to zero (for H–MFI). When raising the initial formaldehyde

concentration, we increased the apparent reaction order up to the first order, and this is clear evidence that the diffusion limitations in the system were partially removed. However, although a higher initial formaldehyde concentration increases the apparent reaction order with respect to formaldehyde precursors up to 1.0, decreasing this initial concentration enhances the buta-1,3-diene selectivity. The apparent activation energy is 20±4 kJ/mol for H–BEA and 26±0.6 kJ/mol for H–MFI. These activation energies are typical of reactions in the diffusion region, with the reaction itself likely occurring in the intradiffusion or transition region. The evaluated Thiele modulus and effectiveness factor showed the reaction being strongly diffusion-limited (the E value ranging from 0.98 to about 1). In liquid-phase condensation, the diffusion limitation is a factor that can conceivably be adjusted to control the process selectivity.

AUTHOR INFORMATION

S.P. Bedenko, ORCID: https://orcid.org/0000-0001-8926-0818

K.I. Dement'ev, ORCID: https://orcid.org/0000-0002-8102-8624

V.F. Tret'yakov, ORCID: https://orcid.org/0000-0001-8891-0866

FUNDING

CONFLICT OF INTEREST

The authors declare no conflict of interest requiring disclosure in this article.

OPEN ACCESS

REFERENCES

1. Bedenko, S.P., Dement'ev, K.I., Tret'yakov, V.F., and Maksimov, A.L., *Petrol. Chem.*, 2020, vol. 60, no. 7, pp. 723–730.
https://doi.org/10.1134/S0965544120070026

2. Cavani, F., Albonetti, S., Basile, F., and Gandini, A., *Chemicals and Fuels from Bio-Based Building Blocks*, Weinheim: Wiley-VCH, 2016.

3. Zacharopoulou, V. and Lemonidou, A.A., *Catalysts*, 2018, vol. 8, no. 1, p. 2.
https://doi.org/10.3390/catal8010002

4. Khadzhiev, S.N., Magomedova, M.V., and Peresypkina, E.G., *Petrol. Chem.*, 2014, vol. 54, no. 4, pp. 245–269.
https://doi.org/10.1134/S0965544114040057

5. Meunier, N., Chauvy, R., Mouhoubi, S., Thomas, D., and De Weireld, G., *Renew. Energy*, 2020, vol. 146, pp. 1192–1203.
https://doi.org/10.1016/j.renene.2019.07.010

6. Sheldon, R.A., Arends, I., and Hanefeld, U., *Green Chemistry and Catalysis*, Weinheim: Wiley–VCH, 2007.

7. Songsiri, N., Rempel, G.L., and Prasassarakich, P., *Catal. Lett.*, 2019, vol. 149, no. 9, pp. 2468–2481.
https://doi.org/10.1007/s10562-019-02837-0

8. Yadav, M.K. and Jasra, R.V., *Catal. Commun.*, 2006, vol. 7, no. 11, pp. 889–895.
https://doi.org/10.1016/j.catcom.2006.04.002

9. Fei, Z., Ai, S., Zhou, Z., Chen, X., Tang, J., Cui, M., and Qiao, X., *J. Ind. Eng. Chem.*, 2014, vol. 20, no. 6, pp. 4146–4151.
https://doi.org/10.1016/j.jiec.2014.01.013

10. Songsiri, N. and Rempel, G.L., *Mol. Catal.*, 2017, vol. 439, pp. 41–49.
https://doi.org/10.1016/j.mcat.2017.06.002

11. Zhang, R., Zhu, H., Xu, S., and Luo, X., *React. Kinet. Mech. Catal.*, 2019, vol. 128, no. 1, pp. 413–425.
https://doi.org/10.1007/s11144-019-01643-4

12. Dumitriu, E., Gongescu, D., and Hulea, V., *Stud. Surf. Sci. Catal.*, 1993, vol. 78, pp. 669–676.

13. Dumitriu, E., Hulea, V., Hulea, T., Chelaru, C., and Kaliaguine, S., *Stud. Surf. Sci. Catal.*, 1994, vol. 84, pp. 1997–2004.

14. Dumitriu, E., Trong On, D., and Kaliaguine, S., *J. Catal.*, 1997, vol. 170, no. 1, pp. 150–160.
https://doi.org/10.1006/jcat.1997.1745

15. Dumitriu, E., Hulea, V., Fechete, I., Catrinescu, C., Auroux, A., Lacaze, J.-F., and Guimon, C., *Appl. Catal. A: Gen.*, 1999, vol. 181, no. 1, pp. 15–28.
https://doi.org/10.1016/S0926-860X(98)00366-4

16. Vasiliadou, E.S., Gould, N.S., and Lobo, R.F., *ChemCatChem.*, 2017, vol. 9, no. 23, pp. 4417–4425.
https://doi.org/10.1002/cctc.201701315

17. Vasiliadou, E.S., Li, S., Caratzoulas, S., and Lobo, R.F., *Catal. Sci. Technol. Royal Society of Chemistry*, 2018, vol. 8, no. 22, pp. 5794–5806.
https://doi.org/10.1039/C8CY01667D

18. Ponomareva, O.A., Chistov, D.L., Kots, P.A., and Ivanova, I.I., *Petrol. Chem.*, 2019, vol. 59, no. 7, pp. 711–718.
https://doi.org/10.1134/S0965544119070156

19. Bedenko, S.P., Kozhevnikov, A.A., Demen'tev, K.I., Tret'yakov, V.F., and Maximov, A.L., *Catal. Commun.*, 2020, vol. 138. 105965.
https://doi.org/10.1016/j.catcom.2020.105965

20. Yu, X., Zhang, Y., Liu, B., Ma, H., Wang, Y., Bao, Q., and Wang, Z., *Chem. Res. Chinese Univ.*, 2018, vol. 34, no. 3, pp. 485–489.
https://doi.org/10.1007/s40242-018-7236-9

21. Bedenko, S.P., Dement'ev, K.I., and Tret'yakov, V.F., *Catalysts*, 2021, vol. 11, no. 10, p. 1181.
https://doi.org/10.3390/catal11101181

22. Plate, N.A. and Slivinskii, E.V., *Osnovy khimii i tekhnologii monomerov* (Fundamentals of Chemistry and Technology of Monomers), Moscow: Nauka, 2002.

23. Arundale, E. and Mikeska, L.A., *Chem. Rev.*, 1952, vol. 51, no. 3, pp. 505–555.

24. Sangthong, W., Probst, M., and Limtrakul, J., *J. Mol. Struct.*, 2005, vol. 748, nos. 1–3, pp. 119–127.
https://doi.org/10.1016/j.molstruc.2005.03.020

25. Choomwattana, S., Maihom, T., Khongpracha, P., Probst, M., and Limtrakul, J., *J. Phys. Chem. C*, 2008, vol. 112, no. 29, pp. 10855–10861.
https://doi.org/10.1021/jp8021437

26. Wannakao, S., Khongpracha, P., and Limtrakul, J., *J. Phys. Chem. A*, 2011, vol. 115, no. 45, pp. 12486–12492.
https://doi.org/10.1021/jp205985v

27. Fu, H., Xie, S., Fu, A., and Ye, T., *Comput. Theor. Chem.*, 2012, vol. 982, pp. 51–57.
https://doi.org/10.1016/j.comptc.2011.12.010

28. Kots, P.A., Artsiusheuski, M.A., Grigoriev, Y.V., and Ivanova, I.I., *ACS Catal.*, 2020, vol. 10, no. 24, pp. 15149–15161.
https://doi.org/10.1021/acscatal.0c03282

29. Dement'ev, K.I., Palankoev, T.A., Kuznetsov, P.S., Abramova, D.S., Romazanova, D.A., Makhin, D.Yu., and Maximov, A.L., *Petrol. Chem.*, 2020, vol. 60, no. 1, pp. 30–38.
https://doi.org/10.1134/S0965544120010065

30. Aramendía, M.A., Borau, V., Jimenez, C., Marinas, J.M., Romero, F.J., and Urbano, F.J., *Catal. Lett.*, 2001, vol. 73, nos. 2–4, pp. 203–206.
https://doi.org/10.1023/A:1016624916214

31. Gao, F., Walter, E.D., Karp, E.M., Luo, J., Tonkyn, R.G., Kwak, J.H., Szanyi, J., and Peden, C.H.F., *J. Catal.*, 2013, vol. 300, pp. 20–29.
https://doi.org/10.1016/j.jcat.2012.12.020

32. Parikh, P.A., Subrahmanyam, N., Bhat, Y.S., and Halgeri, A.B., *Chem. Eng. J. Biochem. Eng. J.*, 1994, vol. 54, no. 2, pp. 79–85.
https://doi.org/10.1016/0923-0467(93)02818-h

33. Villa, A.L., Correa, L.F., and Alarcón, E.A., *Chem. Eng. J.*, 2013, vols. 215–216, pp. 500–507.
https://doi.org/10.1016/j.cej.2012.11.030

34. Schnee, J. and Gaigneaux, E.M., *Catal. Sci. Technol.*, 2017, vol. 7, no. 4, pp. 817–830.
https://doi.org/10.1021/acs.jpcc.6b11248

35. Shi, Z., Arora, S.S., Trahan, D.W., Hickman, D., and Bhan, A., *Chem. Eng. J.*, 2021, p. 134229.
https://doi.org/10.1016/j.cej.2021.134229